ELSEVIER

International Journal of Mass Spectrometry 204 (2001) 55–75

International Journal of Mass Spectrometry

Investigating the effect of transition metal ion oxidation state on oligodeoxyribonucleotide binding by matrix-assisted laser desorption/ionization Fourier transform ion cyclotron resonance mass spectrometry

Robert L. Hettich

Chemical and Analytical Sciences Division, Oak Ridge National Laboratory, Oak Ridge, TN 37831-6365, USA

Received 9 March 2000; accepted 27 July 2000

Abstract

Investigations of the interactions of metals with nucleotides and oligonucleotides are important for a variety of areas, including understanding nucleic acid metabolism and ability of the metals to stabilize or destablize the double-stranded helix of DNA. This report illustrates the application of matrix-assisted laser desorption/ionization Fourier transform ion cyclotron resonance mass spectrometry for the study of the fundamental interactions of metal ions with small, single-stranded oligonucleotides, with a specific focus on evaluation of sequential metal ion attachment and binding site(s) determination. Whereas incorporation of Cu (I) into dinucleotides reveals the maximum number of protons that can be replaced by singly charged metal ions, incorporation of iron (II, III) into the same biomolecules is sensitive to steric binding factors as well. These results suggest a mechanism in which complexes of the metal ion and the laser matrix compound (2,5-dihydroxybenzoic acid, or DHB) coordinate with the oligonucleotides and attach metal ions by eliminating neutral DHB molecules. Ions of divalent (Zn^{2+}, Fe^{2+}), trivalent (Fe^{3+}, Ce^{3+}), and tetravalent (Ce^{4+}, Th^{4+}) metals all bind strongly to oligonucleotides and are retained even in the fragment ions. Based on high-resolution mass measurements and fragmentation information, structures are proposed for these gas phase species in which the metal ion coordination to the oligonucleotide involves both phosphate and nucleobase interactions. These studies provide molecular level information about metal ion interactions with oligonucleotides, and may be the basis for determining how certain metal ions can be exploited as selective probes for biomolecular structure interrogation. (Int J Mass Spectrom 204 (2001) 55–75) © 2001 Elsevier Science B.V.

Keywords: MALDI FTICR mass spectrometry; Metal ion binding; Oligonucleotides; Transition metal ions

1. Introduction

The interaction of metal ions with biomolecules such as proteins and DNA is essential for many critical biological processes. The metal ions stabilize higher order biological structures, and thus help modulate biological activity. Metal ions can also have deleterious effects on biological systems, sometimes induced by simply varying the concentration of the metal species [1]. Because of the importance of DNA and RNA function in cellular systems, understanding the interaction of metals and their complexes with these biomolecules has become a central question in molecular biology.

* E-mail: hettichrl@ornl.gov

PII S1387-3806(00)00338-9

It is well known that metal ions and nucleotides are involved in the basic metabolic processes of life [2,3]. This is due at least in part to the role that metal ions play in stabilizing the self-association of nucleotides [4]. Metal ions also interact strongly with oligonucleotides. For example, divalent metal ions can induce curvature in dinucleotides such that the metal ion is equidistant from the bases at the 5′ and 3′ ends of the dinucleotide [5]. Understanding metal ion interactions with double-stranded oligonucleotides is important for a number of applications, including the antitumor activity of cis-platin (which is thought to be due to intercalation into specific sites in DNA) [6], the application of metals in nonenzymatic DNA hydrolysis, such as Fenton reactions [7–10], and the use of heavy metals in DNA staining for electron microscopy and x-ray crystallography studies [6]. Although much experimental work has been conducted on the coordination chemistry of heavy metals with nucleic acids, uncertainty remains about the fundamental nature of metal ion binding to DNA (such as binding sites and intercalation selectivity). Thus it is important to further characterize metal–nucleotide and oligonucleotide interactions with technology such as mass spectrometry that is capable of probing structures at the molecular level.

Past research has provided information about metal ion binding to single-stranded, small oligonucleotides, although some controversy exists about preferential metal-binding sites. In contrast to the electrostatic affinity of metal ions like Na^+, K^+, Mg^{2+}, and Ca^{2+} for phosphate groups, the transition metals are more likely to form covalent bonds with the nucleobases themselves [11]. The heterocyclic and amidate nitrogen atoms of the nucleobases are well suited to form covalent bonds with the polarizable, heavy metal centers. This results from electron donation by either nitrogen or oxygen atoms of the nucleobases to the unfilled metal orbitals acting as receptors. In general, the most common binding sites for heavy metal ions appear to be the N^7 atoms in adenine and guanine [12]. The hydroxyl group of pentose ring is a poor ligand for metal ion coordination [6]. However, even with these simple guidelines, the wealth of available metal binding sites of a nucleotide leads to a variety of structures [6]. There is no simple rule for determining which metal ions preferentially bind to nucleobases rather than the phosphate groups. With regard to the double-stranded oligonucleotides of DNA, metal ions which bind to the phosphate groups tend to stabilize the double-helix structure, whereas metals that preferentially attach to the nucleobases tend to destabilize the DNA due to competition with Watson-Crick base pairing [13]. The strong affinity of heavy metals for binding to the nucleobases is thought to contribute to the high mutagenicity of these species [6].

Mass spectrometry has become an important tool for studying metal ion–biomolecule systems, including peptides, proteins, and oligonucleotides [14]. The capabilities of mass spectrometry for accurate mass measurement and ion manipulation provide molecular level information about the interactions of metal ions and biomolecules. Although previous reports have discussed the attachment of Fe^{2+} to oligonucleotides [15–17], we have recently described how both Fe^{2+} and Fe^{3+} complexes with oligonucleotides can be generated in the gas phase and identified with Fourier transform ion cyclotron resonance (FTICR) mass spectrometry [18]. This information prompted a more thorough investigation of gas phase metal ion–oligonucleotide systems in general.

The goal of this article is to summarize the application of matrix-assisted laser desorption/ionization (MALDI) FTICR mass spectrometry for the study of the fundamental interactions of metal ions with small, single-stranded oligonucleotides, with a specific focus on evaluation of sequential metal ion attachment and binding site(s) determination. We will begin with a discussion of metal ion dinucleotide interactions, systematically varying either the identity of the metal ion or the sequence of the dinucleotide. This will provide basic information about metal ion interactions with biomolecules containing a limited number of binding sites. These results will be used to evaluate the interaction of oligonucleotides with multivalent metal ions, ranging from divalent (Zn^{2+}, Fe^{2+}), to trivalent (Fe^{3+}, Ce^{3+}), and finally tetravalent (Ce^{4+}, Th^{4+}) species. These studies should help identify the structures and stabilities of gas phase metal ion–oligonucleotide systems, and help determine how closely these systems may correlate with analogous

solution phase structures, in which the solvent is present and may alter the metal ion binding properties. This investigation may also provide information on how multivalent metal ions could be exploited as selective probes for biomolecule interrogation.

2. Experimental

All chemicals were acquired commercially and used without further purification. The nucleotides and dinucleotides were purchased from Sigma Chemical Company (St. Louis, MO), and the larger oligonucleotides were obtained from Pharmacia Biotechnology, Inc. (Piscataway, NJ). The laser matrix compounds 2,5-dihydroxybenzoic acid (DHB) and 3-hydroxypicolinic acid (HPA) were acquired from Aldrich Chemical Company (Milwaukee, WI). The following inorganic salts were used in this study: calcium chloride (Aldrich), cerium (IV) ammonium sulfate (Fisher Scientific), cerium (III) nitrate (J.T. Baker, Phillipsburg, N.J.), cobalt (II) acetate (Aldrich), copper (II) acetate (Aldrich), iron (III) chloride (EM Science, Cherry Hill, N.J.), magnesium chloride (Aldrich), and zinc acetate (EM Science).

Samples for the MALDI experiment were prepared by mixing a few microliters of an aqueous inorganic salt solution ($\sim 10^{-3}$–10^{-2} M) such as iron (III) chloride with the laser matrix solution [$\sim$1.5 M in acetonitrile:water (1:1, v:v)]. For the iron–DHB mixture, the solution turned dark blue in coloration, indicating formation of a complex between the matrix and the iron salt. A few microliters of an aqueous oligonucleotide solution ($\sim 10^{-5}$–10^{-4} M) was then added to this colored solution. The resulting mixture, consisting of a few picomoles of biological analyte with a 10–100-fold molar excess of inorganic salt and a large molar excess of matrix compound, was air dried onto a stainless steel probe tip, which then was inserted into the vacuum chamber of the mass spectrometer and used as the laser desorption target. All mass spectra were acquired with a Finnigan FT/MS 2001 FTICR mass spectrometer, which is configured with a 6 tesla superconducting magnet. Laser desorption/ionization was accomplished with a Laser Photonics LN-1000 nitrogen laser (337 nm). One laser shot was sufficient to generate sufficient ion intensity (either positive or negative ions) to provide a complete mass spectrum; however, in most cases, 5–20 mass spectra were signal-averaged prior to Fourier transformation to improve signal/noise. The laser-generated ions were decelerated [19] to improve trapping in the FTICR cell, and then detected under either medium resolution (broadband detection) or high-resolution (heterodyne detection) conditions. Calibrations for accurate mass measurements were accomplished with known calibrant ions, such as the molecular ion and *w*-type fragment ions from *d*(AGCT). Collisionally-activated dissociation (CAD) experiments were conducted by isolating ions of interest and then accelerating those ions into an argon target gas (static pressure of $\sim 3 \times 10^{-6}$ Torr) under sustained off-resonance irradiation (SORI) conditions [20], employing a frequency 500 kHz lower than the parent ion cyclotron frequency for 100 ms.

3. Results and discussion

Examination of the gas phase complexes of different transition metal ions with dinucleotides of varying sequences provides molecular level information about metal ion–dinucleotide interactions and binding sites. By varying the identity of the metal ions and keeping the dinucleotide constant, it is possible to determine differences in binding due to metal variations. This will be discussed below for various metal ions with the dinucleotide *d*AG. Expanding these results to then probe the interactions of iron and copper with dinucleotides of varying sequences provides a method to investigate the influence of the nucleobase sequences. This information is then used in the study of divalent (zinc, iron), trivalent (iron, lanthanides), and tetravalent (lanthanides, actinides) metal interactions with larger oligonucleotides.

3.1. d*AG–transition metal ion interactions*

The dinucleotide *d*AG provides a variety of acidic protons and possible binding sites for metal ions. By

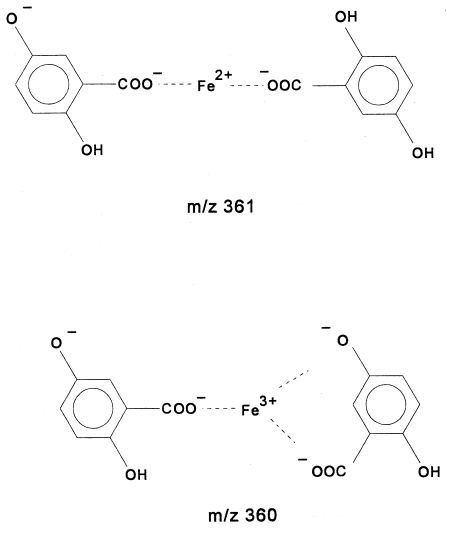

Scheme 1.

varying the identity of the metal ion and keeping the dinucleotide constant, it should be possible to examine what similarities and differences are exhibited in the metal ion–dinucleotide complexes.

Most of the MALDI FTICR mass spectra of iron–DHB–oligonucleotide samples reveal negative ions due to complexes of (iron–DHB), specifically at nominal *m/z* 361, 569, 777, and 985. High-resolution mass measurement of the nominal *m/z* 361 ion packet reveals the presence of $(Fe + DHB_2 - 3H)^-$ at *m/z* 361 as well as $(Fe + DHB_2 - 4H)^-$ at *m/z* 360, corresponding to complexes containing Fe^{2+} and Fe^{3+}, respectively. Possible structures for these ionic species are illustrated in Scheme 1. Ion pairs can be transferred into the gas phase by the laser desorption event, and are known to be stable in the gas phase [21–23]. The higher mass ions mentioned previously would be formed by additional attachment of DHB and iron ions, i.e. $(Fe_x + DHB_{x+1} - yH)^-$. The appearance of these negative ions in the mass spectra suggests that the corresponding neutral ion pairs are likely also to be present in the gas phase. Either of these species may play an important role in the transfer of Fe^{2+} and Fe^{3+} to the oligonucleotides.

Fig. 1 illustrates the negative ion MALDI FTICR mass spectrum of a (*d*AG + $FeCl_3$ + DHB) sample. Abundant negative ions are observed at *m/z* 579, 633, 786, and 841. The *m/z* 579 ion is the deprotonated dinucleotide $(M-H)^-$, and was used as an internal calibrant ion. Expansion of the metal-containing molecular ion region, shown in the insert of Fig. 1, reveals an abundant ion at *m/z* 633 corresponding to $(dAG+Fe-3H)^-$, which contains iron as Fe^{2+}. The isotopic signature closely matches the expected iron and carbon contributions for this species. Although the $(M-H)^-$ ion at *m/z* 579 dissociates readily by nucleobase and/or deoxynucleoside elimination, attempts to collisionally dissociate the *m/z* 633 ion were largely unsuccessful. Virtually no fragment ions were observed prior to ion ejection from the cell at high translational energies. The implication from these results is that the metal ion stabilizes the dinucleotide with respect to dissociation, possibly by tethering the two nucleobases together. Such a structure would require at least two bond cleavages to generate fragment ions. This postulation is based on the observation that Hg^{2+} binds to DNA at pH 9 by releasing two protons per Hg^{2+} to generate base–base cross linking [11]. The ion at *m/z* 786 in Fig. 1 corresponds to $(dAG+Fe+DHB-4H)^-$, and presumably is generated by reaction of a $(Fe^{3+}+DHB_2)$ species with *d*AG. Transfer of a proton from *d*AG to the $(Fe^{3+}+DHB_2)$ complex would result in elimination of a neutral DHB molecule, and would then leave a $(Fe^{3+}+DHB)$ species attached to the dinucleotide. Two additional protons would have to be abstracted from the dinucleotide to eliminate the remaining DHB molecule. If this level of proton abstraction is not possible, then the second DHB moiety cannot be eliminated and remains in the complex. The ion at *m/z* 841 likely is due to subsequent reaction of *m/z* 633 with another $(Fe^{2+}+DHB_2)$ molecule to liberate one molecule of DHB. For this complex, both DHB molecules apparently cannot be eliminated to generate a $(dAG+2Fe-5H)^-$ complex at *m/z* 687. This suggests that even though there may be additional acidic hydrogens present in the dinucleotide, they cannot be accessed by the attached (iron+DHB) group to eliminate the second neutral DHB molecule from the complex. The presence of an abundant ion at *m/z* 840 implies a similar reaction of $(Fe^{3+}+DHB_2)$ with the *m/z* 633 ion as well. The higher mass ions apparent in

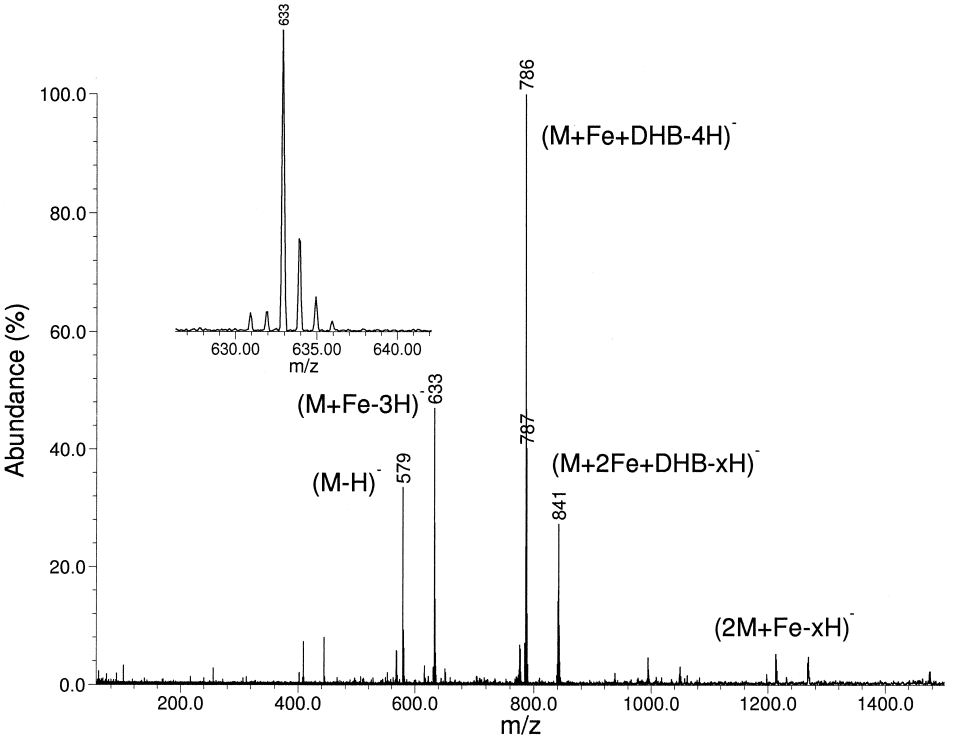

Fig. 1. Negative ion MALDI FTICR mass spectrum of sample containing 2,5-DHB, iron (III) chloride, and *d*AG. The inset is an expansion of the $(M+Fe-xH)^-$ ion, revealing the presence of only Fe^{2+} in this species.

Fig. 1 correspond to additional attachment of (iron+DHB) complexes to the lower mass precursor ions. This would be expected, based on the discussion given above about the observation of these higher mass (iron+DHB) species in the mass spectra. Fig. 1 also reveals an appreciable abundance of an iron-containing *d*AG dimer $(2dAG+Fe-4H)^-$ observed at *m/z* 1212. The abundance of this species could be enhanced by increasing the concentration of the dinucleotide in the sample, although no attempt was made to quantitatively investigate this effect. Metal-bound dinucleotide dimers were observed for most of the other metals examined in this section. For comparison, the deprotonated *d*AG dimer at *m/z* 1159 is not observed. Although $(Fe^{3+}+DHB_2)^-$ ions are observed readily in the mass spectra, no $(dAG+Fe-4H)^-$ is observed (this ion would contain Fe^{3+}). Because of the inability to abstract a third proton from a single *d*AG molecule, it might be easier for the $(Fe^{3+}+DHB_2)$ system to tether two *d*AG molecules together, thereby permitting formation of an iron+*d*AG dimer concomitant with the elimination of both DHB molecules.

Similar complexes were observed for zinc and *d*AG. In this case, the most abundant negative ion was *m/z* 641 $(dAG+Zn-3H)^-$, corresponding to Zn^{2+}. High-resolution mass measurement confirmed the presence of zinc, with its diagnostic isotopic distribution, in this nominal *m/z* 641 ion. Zinc+DHB ions at *m/z* 585, 801, and 1017 were observed as well, and correspond to analogous ions as those discussed for the iron+DHB system above (as expected, the zinc is observed to be divalent in all of these species). The presence of negative ions corresponding to $(dAG+Zn+DHB-3H)^-$ at *m/z* 795 and $(dAG+2Zn+DHB-5H)^-$ at *m/z* 857 suggest that the (zinc+DHB) complexes assist in the transfer of zinc to the dinucleotide much like the iron system discussed previously. The presence of a metal-bound *d*AG dimer $(2dAG+Zn-3H)^-$ at *m/z* 1221 is also noted

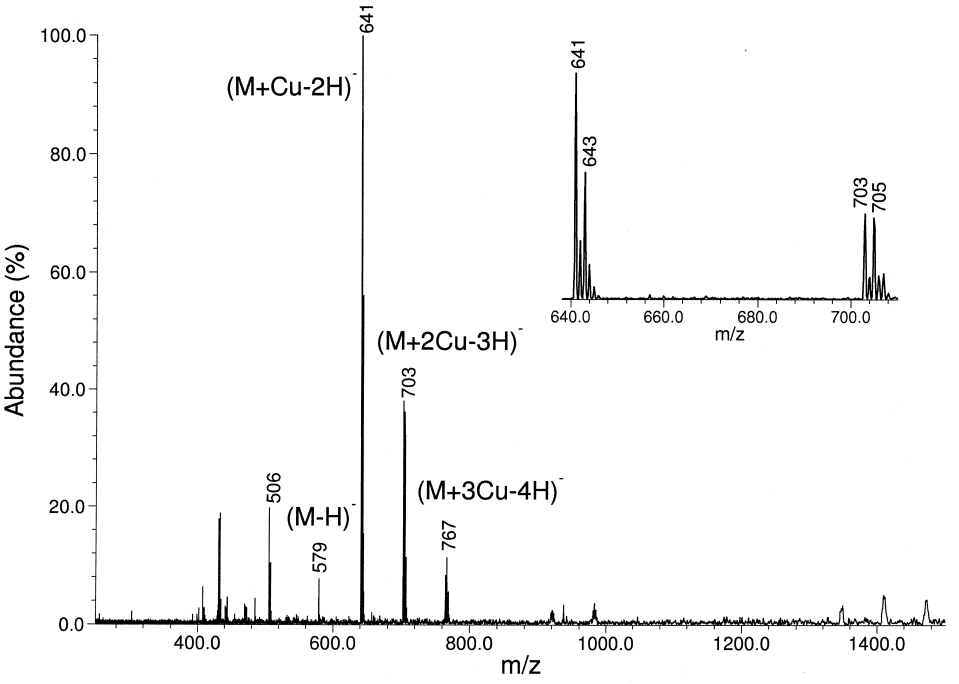

Fig. 2. Negative ion MALDI FTICR mass spectrum of sample containing 2,5-DHB, copper (II) acetate, and *d*AG. The insert is an expansion of the *m/z* 640–725 region, revealing the isotopic distributions of the copper-containing ions.

for this system. The positive ion mass spectrum reveals similar ions, with the most abundant ion at *m/z* 643 corresponding to $(dAG+Zn-H)^+$.

Copper yields quite different results under these same experimental conditions. Up to three copper ions can be attached to the *d*AG dinucleotide, as shown in Fig. 2. Only a small abundance of $(dAG+Cu+DHB-xH)^-$ ions are observed in this case. Further, high-resolution measurements reveal that copper is present only as Cu^+ in the *m/z* 641, 703, and 765 isotopic clusters, as shown in the insert of Fig. 2. It is somewhat surprising that no Cu^{2+} is observed in the complexes, since copper (II) salt was used in the sample preparation. However, as was observed in the iron studies [18], the laser desorption event produces stable ion pairs in the gas phase which may not reflect exactly the oxidation states of the metals that originally were added to the sample. The copper ion appears to act similar to the alkali metal ions, and simply displaces acidic protons of the dinucleotide. Collisional dissociation of the *m/z* 641 ion revealed loss of adenine and deoxyadenosine as the primary fragment products. In no case was the copper ion lost in the dissociation. Collisional dissociation of the *m/z* 703 ion $(dAG+2Cu-3H)^-$ also revealed loss of deoxyadenosine, verifying the presence of both copper ions in the remaining fragment ion. Collisional dissociation could not be conducted on the $(dAG+3Cu-4H)^-$ species due to its low abundance in the mass spectra. These fragmentation results indicate that at least two copper ions are associated strongly with the deoxyguanosine, replacing the 3′ hydroxyl proton and/or the nucleobase protons. The most likely binding site is the guanine nucleobase, based on the fact that the guanine has a high affinity for a similar metal ion, Ag^+, which chelates to the N^7–O^6 positions of guanine, bringing the nucleobase into the enol tautomer [11]. In order to examine this metal ion binding site issue in greater detail, the interaction of copper with dinucleotides of varying sequences will be discussed in the Sec.3.2.

Other divalent metal ions also could be attached to

Table 1
Copper ion addition to dinucleotide negative ions[a]

Dinucleotide	Maximum number of copper ions attached
*d*TG	3
*d*CA	2
*d*CT	2
*d*GG	4
*d*AG	3

[a] Copper (II) acetate was mixed with the aqueous DHB matrix, and then the dinucleotide was added to the solution. The resulting mixture was dried onto the stainless steel probe tip for MALDI-FTICR-MS examination. Each copper added replaces one proton of the dinucleotide.

*d*AG. $(d\text{AG}+\text{metal}-3\text{H})^-$ ions were observed for cobalt, calcium, and magnesium by addition of the appropriate salts to the DHB matrix solution. For both calcium and magnesium, the $(d\text{AG}+\text{metal}-3\text{H})^-$ ions were observed in very low abundances, whereas much higher abundances of $(d\text{AG}+\text{metal}-\text{H})^+$ ions were observed in both cases. This result is consistent with the fact that both magnesium and calcium prefer binding to the phosphate groups, and have relatively little affinity for the nucleobases [11]. A moderate amount of $(d\text{AG}+\text{Co}-3\text{H})^-$ negative ions could be generated, as expected since this metal ion is similar to iron. No Co^{3+} was observed in the $(d\text{AG}+\text{Co}-x\text{H})^-$ complex.

3.2. Iron– and copper–dinucleotide complexes

To investigate how the metal ion–dinucleotide complex depends on nucleobase identity, a series of different dinucleotides was examined with iron and copper salts. Based on the observation of copper (I) addition to *d*AG discussed previously, several different sequences were examined to probe the number and location of replaceable protons. As stated previously, up to three protons can be replaced by copper ions for *d*AG. In contrast, only a maximum of two copper ions can be added to *d*CA. Table 1 summarizes the results obtained for five different dinucleotides, and reveals that between two and four copper ions can be added to a given dinucleotide, depending on the sequence. The minimum number of copper additions (2) is observed for *d*CA and *d*CT, whereas up to four coppers can be added to *d*GG. Because copper is present in all of these complexes as Cu^+, it does not require multisite attachment like the other multivalent metal ions examined in this article, and thus behaves like an alkali metal and simply replaces available acidic hydrogens in the dinucleotides. This enables copper to be used to evaluate the maximum number of dinucleotide protons that can be replaced by a singly charged metal ion. The data in Table 1, along with dissociation information of copper-containing fragment ions, suggest that copper ions primarily replace acidic hydrogens on the nucleobases of the dinucleotides. Because the metal ion coordination appears to be dependent primarily on the identity of the nucleobases, the relative involvement of the 3′-deoxyribose hydroxy groups in metal ion binding seems to be minimal. For comparison, H/D exchange reactions of nucleotides with D_2O or D_2S show extensive proton abstraction, revealing that the protons of the hydroxyl groups can compete with the amine hydrogens for exchange [24]. The experimental data indicates that copper is able to replace two protons on a guanine nucleobase, and only one proton on each of the other nucleobases. Thus, the first copper (I) ion added to *d*CA might occur by proton abstraction from one of the exocyclic amino groups of either adenine or cytidine and subsequent replacement by Cu^+. The second copper (I) ion would be added to the exocyclic amino group of the other nucleobase. The addition of copper (I) ions to *d*AG would occur by attachment of up to two copper ions on guanine and the third copper on adenine, yielding the structure shown in Scheme 2a. Based on the results known for Ag^+ attachment to guanine, an alternate resonance structure could be proposed, as shown in Scheme 2b, in which one of the copper (I) ions is coordinated to the O^6 and N^7 positions of guanine. It would be possible to attach up to two copper (I) ions to each guanine nucleobase in *d*GG, again supporting the results shown in Table 1. In general, this copper (I) attachment model exploits the same nucleobase acidic protons that are involved in Watson-Crick base pairing in DNA.

Based on the information of total number of dinucleotide protons that can be replaced by metal

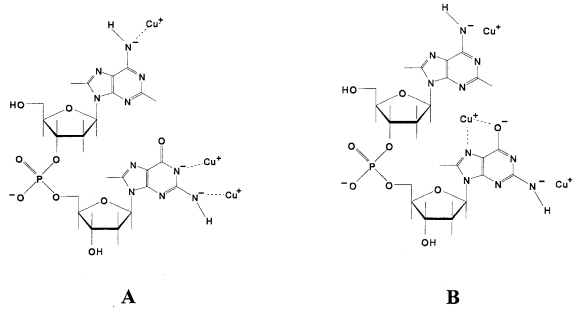

Scheme 2.

ions (as determined by copper ion attachment), the interactions of iron with the same dinucleotides listed above was examined to investigate how a multivalent metal ion would coordinate with the dinucleotides. Table 2 lists the results for iron. In this case, iron can exist as either Fe^{2+} or Fe^{3+}, dependent not only on the number of replaceable protons, but also the steric factors involved in the coordination of the multivalent metal ion to at least two sites in the dinucleotide. Only Fe^{2+}-containing complexes are seen for *d*TG, *d*CA, and *d*AG, whereas both Fe^{2+} and Fe^{3+} are observed for the *d*GG system, as evidenced by the appearance of both *m/z* 648 and 649 in Fig. 3. No evidence is present for multiple iron ion attachment without DHB present to any of these dinucleotides, which supports the data in Table 1 for the maximum number of abstractable protons. The *d*CT system does not contain a $(d\mathrm{CT}+\mathrm{Fe}-3\mathrm{H})^-$ ion; rather only a $(d\mathrm{CT}+\mathrm{Fe}+\mathrm{DHB}-3\mathrm{H})^-$ ion is observed. Inspection of Table 1 reveals that two protons can be replaced by copper (I) for *d*CA negative ions, so $(d\mathrm{CA}+\mathrm{Fe}-3\mathrm{H})^-$ would be expected but not $(d\mathrm{CA}+\mathrm{Fe}-4\mathrm{H})^-$. This is in accord with the experimental observations. Both *d*TG and *d*AG have three removable protons, yet only Fe^{2+} complexes are observed. This may imply that steric restrictions preclude coordination of a multivalent Fe^{3+} metal ion to these dinucleotides, as will be discussed below. *d*GG has four removable protons, so both Fe^{2+} and Fe^{3+}–dinucleotide complexes would be expected. Again, this is in agreement with the experimental results. Two protons can be abstracted from *d*CT, yet only a $(d\mathrm{CT}+\mathrm{Fe}+\mathrm{DHB}-3\mathrm{H})^-$ is observed in the negative ion mass spectrum. The iron coordination results for *d*TG, *d*AG, and *d*CT may imply that nucleobase stacking occurs within these dinucleotides to generate structures in which the abstractable protons are too far apart to permit interaction with a single metal ion. For example, solution phase studies of nucleotides indicate that purine–purine base stacking is known to be more favorable than purine–pyrimidine, which in turn is more stable than pyrimidine–pyrimidine [13]. Even with poor nucleobase stacking orientations in the dinucleotides, one Fe^{2+} ion could still interact exclusively with the guanine nucleobase of *d*TG and *d*AG. The absence of a guanine nucleobase and the lack of strong base–base interactions for pyrimidines may result in a greater separation distance between the cytidine and thymidine nucleobases of *d*CT, and reduce the possibility of base–base cross-linking by Fe^{2+}.

Table 2
Iron ion addition to dinucleotide negative ions[a]

Dinucleotide	Maximum number of iron ions added
*d*TG	1 (Fe^{2+} only)
*d*CA	1 (Fe^{2+} only)
*d*CT	0 (only $(dCT + Fe + DHB\text{-}3H)^-$ observed)
*d*GG	1 (both Fe^{3+} and Fe^{2+} present)
*d*AG	1 (Fe^{2+} only)

[a] Iron (III) chloride was mixed with the aqueous DHB matrix, and then the dinucleotide was added to the solution. The resulting mixture was dried onto the stainless steel probe tip for MALDI-FTICR-MS examination. Each Fe^{2+} added replaces two protons of the dinucleotide; each Fe^{3+} replaces three protons.

3.3. Structures and formation of the metal ion–dinucleotide complexes

The experimental data discussed previously suggests that the nucleobases are strongly involved in the metal binding from these dinucleotides. Because the deprotonated dinucleotide ion does not have the hydrogen ion on the phosphate group, the only sources of acidic protons are the 3′-deoxyribose hydroxy groups and amino groups of the nucleobases. Because the attachment of copper and iron ions to dinucleotides is dependent primarily on the nucleobase identities, it appears that the protons of the

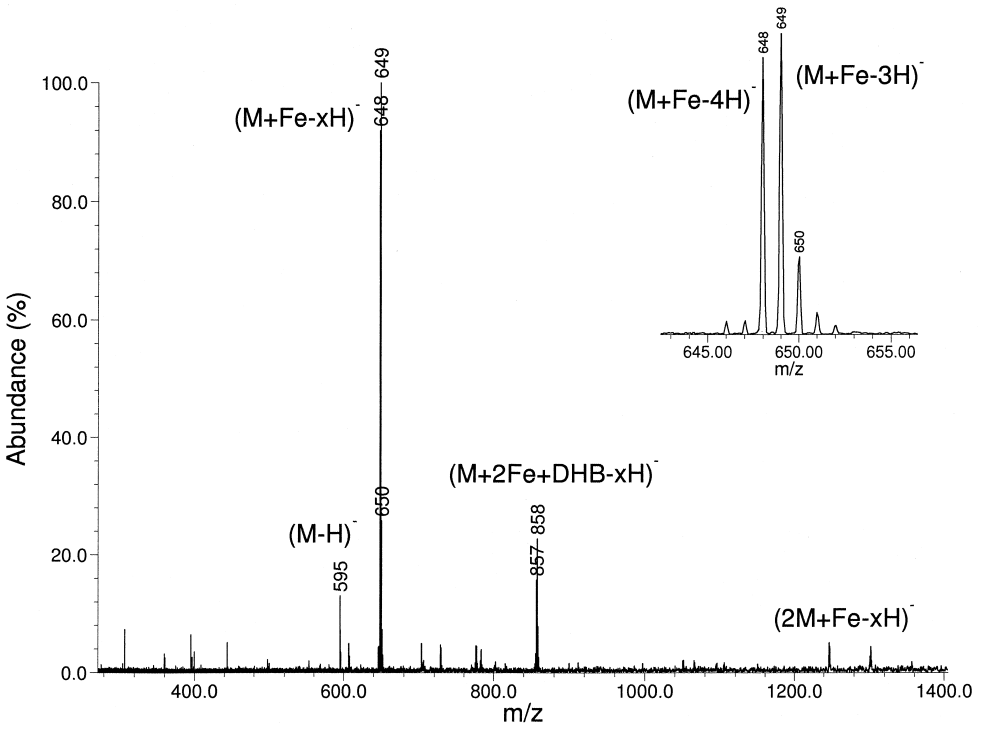

Fig. 3. Negative ion MALDI FTICR mass spectrum of sample containing 2,5-DHB, iron (III) chloride, and *d*GG. The insert is an expansion of the $(M+Fe-xH)^-$ ion, revealing the presence of both Fe^{2+} (*m/z* 649) and Fe^{3+} (*m/z* 648) in this species.

deoxyribose hydroxyl groups are relatively uninvolved in metal ion binding.

For the metal–dinucleotide negative ions such as $(d\text{CA}+\text{Fe}-3\text{H})^-$, one plausible structure consistent with the high resolution mass measurement and fragmentation data is shown in Scheme 3. For this species, one proton has been removed from each of the exocyclic amino groups of the cytidine and adenine nucleobases, and the divalent metal ion is coordinated to each nucleobase. Although this species is drawn as ionic, it is likely that the transition metal ion coordination to the nucleobases in this case is mostly covalent in nature. The deprotonated exocyclic amine serves as an excellent ligand for heavy metal coordination; however, it is unlikely that this mode of binding is representative of reaction products in neutral aqueous solutions [6]. Clearly, several alternate resonance structures could be proposed in which the metal ion is coordinated to each nucleobase. The number of abstractable protons, and thus the nature of the metal ion binding, obviously is dependent on the identities of the nucleobases in the dinucleotide. For compounds such as *d*AG, several possibilities exist for metal ion coordination; two likely structures are shown in Scheme 4 for $(d\text{AG}+\text{Fe}-3\text{H})^-$. Based on the iron ion attachment results and fragmentation data

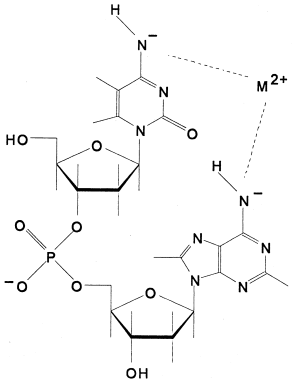

Scheme 3.

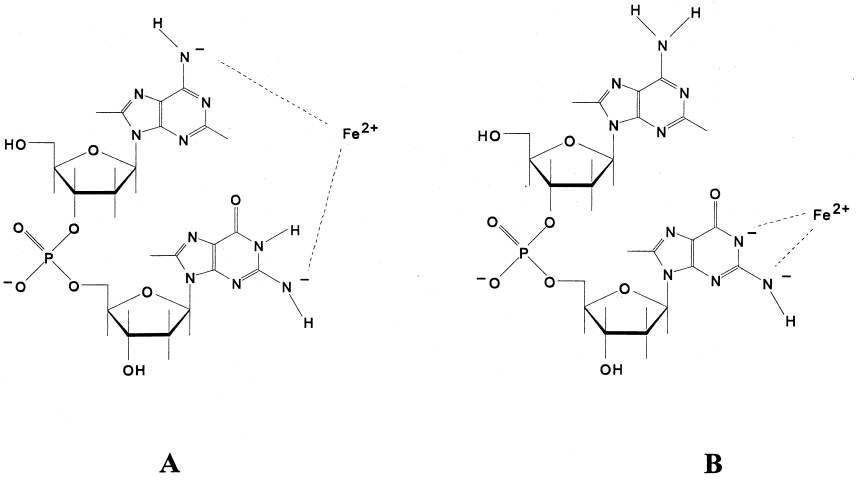

Scheme 4.

for *d*TG, *d*AG, and *d*GG, the most likely structure appears to be Scheme 4b (once again, a related tautomeric enol ion in which the iron is coordinated to the O^6 instead of the N^1 position of the guanine could be proposed in this case). The ability to coordinate Fe^{2+} completely with the guanine nucleobase is also supported by the observation of $(dGG+Fe-4H)^-$, whose possible structure is depicted in Scheme 5. The structures proposed in the schemes are based exclusively on experimental information from the mass spectra. For these small systems, semi-empirical molecular modeling with ZNDO parameters could also be used to predict structures and crude energetics for comparision against the experimental data. This work is in progress for the metal ion–dinucleotide systems.

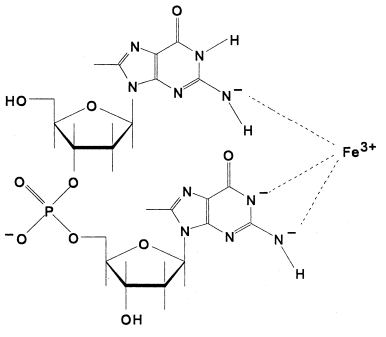

Scheme 5.

Based on the experimental data shown previously, one possible mechanism for the formation of the metal ion–oligonucleotide species by MALDI FTICR mass spectrometry is discussed below and shown in Scheme 6. The laser desorption/ionization event produces gas phase iron–DHB complexes (for both Fe^{2+} and Fe^{3+}), which may be present as the ions as illustrated in Scheme 1, or as charge-balanced ion pairs. The electron-rich heteroatoms of the dinucleotide provide an excellent initial interaction site for the iron+DHB ion-pair complexes. Coordination of the iron+DHB complexes to a heteroatom which is adjacent to acidic protons would lead to favorable conditions for elimination of DHB with concomitant attachment of the iron ion. Thus, it would be possible for the $(Fe^{2+}+DHB_2)$ complex to interact with an exocyclic amino group of the dinucleotide, as shown in step 1 of Scheme 6. An intermediate could be formed, as shown in step 2 of Scheme 6, in which the iron ion is associated with the electronegative nitrogen atom of the exocyclic amino group. Hydrogen bonding between the amino hydrogen of the dinucleotide and the carbonyl oxygen of the dihydroxybenzoic acid would assist the transfer of a proton from the dinucleotide to the DHB. Elimination of a neutral molecule of DHB would then leave the $(Fe^{2+}+DHB)$ complex attached to the dinucleotide, as shown in step 3. Abstraction of another

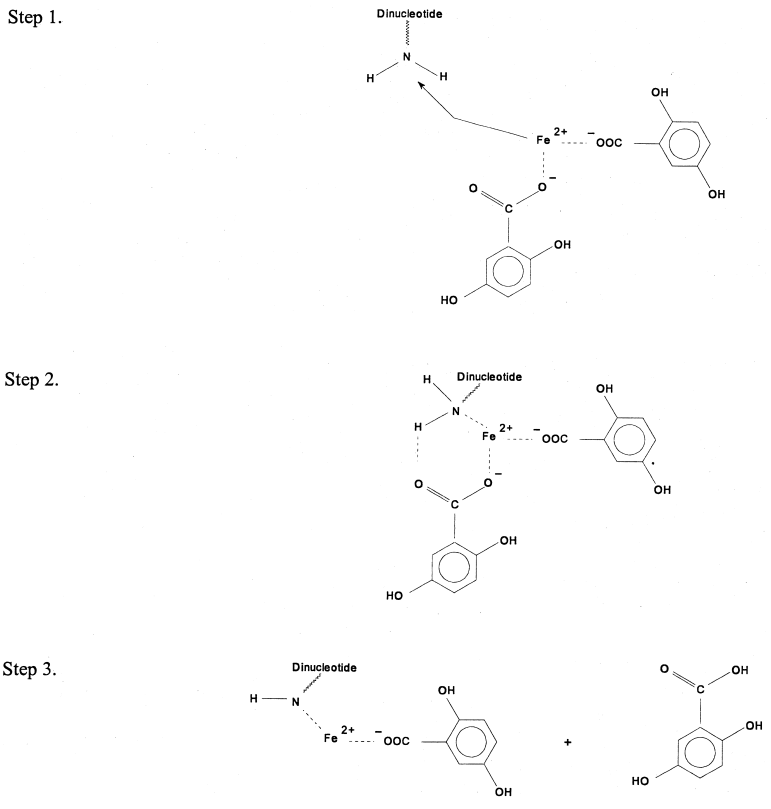

Scheme 6.

proton from the dinucleotide (possibly from the other nucleobase) would liberate the remaining DHB and leave a (dinucleotide+Fe−3H)$^-$ species. It is clear that at least two critical steps are required for this process; (1) the iron+DHB complex must coordinate to the dinucleotide, and (2) one or more protons must be abstracted to eliminate neutral DHB molecules and attach the metal ion. Obviously the $Fe^{3+}+DHB_2$ complex shown in Scheme 1 could attach to the dinucleotide as well. If three protons cannot be removed, then the resulting complexes will consist of (dinucleotide+Fe+DHB−4H)$^-$, as is evidenced in Fig. 1. The observation of (dinucleotide+metal ion+DHB) species supports the involvement of the matrix compound in the transfer of the iron to the oligonucleotide.

3.4. Divalent metal ion–oligonucleotide interactions: zinc

It has been previously shown that abundant iron–ATP adducts can be generated by this MALDI FTICR mass spectrometry process in which a metal salt is doped into the laser matrix [18]. In that case, the ions were primarily (ATP+Fe−4H)$^-$ corresponding to Fe^{3+}, with a smaller amount of (ATP+Fe−3H)$^-$, representing Fe^{2+}. We wanted to evaluate how Zn^{2+} would coordinate with ATP and whether multiple zinc ions could be attached. The MALDI FTICR mass spectra of ATP mixed with zinc revealed an abundant (ATP+Zn−3H)$^-$ ion at nominal *m/z* 568. High-resolution mass measurement of *m/z* 568 indicated the expected isotopic pattern for one zinc atom. A fragment ion was observed at *m/z* 550, and corresponds to H_2O loss from the *m/z* 568 ion (the zinc ion is still retained in the fragment, even though a neutral molecule of water had been eliminated). Although this result may be somewhat surprising if the zinc ion is assumed to be coordinated exclusively by deprotonation of the phosphate groups, it is supported by Raman spectroscopy data that suggest that deprotona-

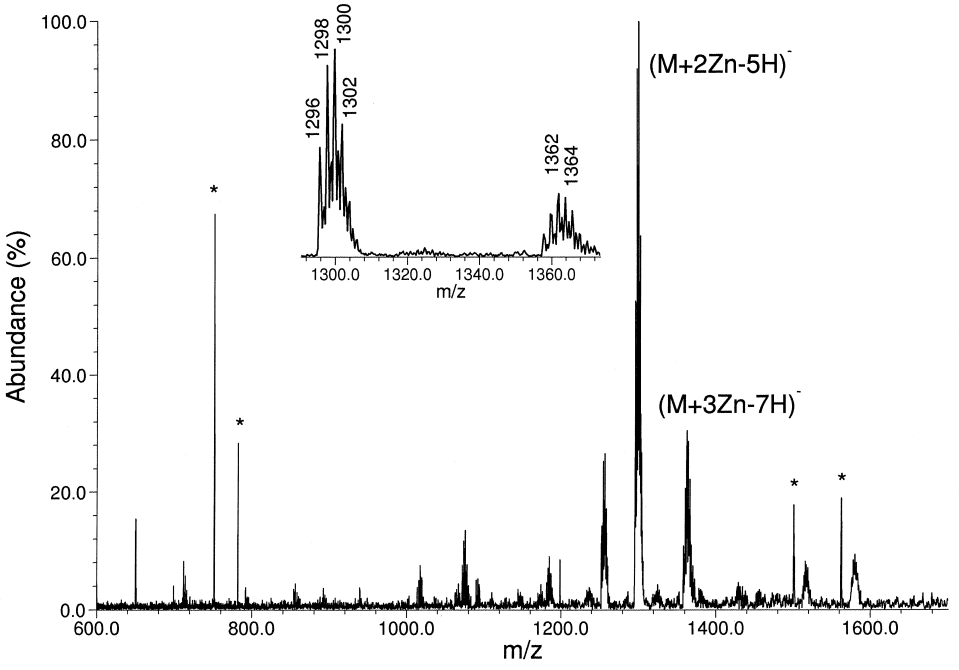

Fig. 4. Negative ion MALDI FTICR mass spectrum of sample containing 2,5-DHB, zinc (II) acetate, and *d*ACGT. The insert is an expansion of the *m/z* 1275–1375 region, revealing the isotopic distributions of the dACGT ions containing two and three zinc ions. The peaks marked with an asterisk (*) are noise spikes that were determined to arise from the ion gauge.

tion of the adenine nucleobase is involved in Zn^{2+} binding to ATP in solution [13]. There is no evidence for the addition of a second zinc to form a $(ATP+2Zn-5H)^-$ ion. The presence of (zinc+DHB) negative ions along with the observation of ions for $(ATP+Zn+DHB-3H)^-$ at *m/z* 722 and $(ATP+2Zn+DHB-5H)^-$ at *m/z* 784 support a similar metal ion transfer mechanism for zinc as that proposed for iron in Scheme 6 (except no trivalent zinc is possible in this case). The positive ion mass spectrum revealed similar ions, with an abundant $(ATP+Zn-H)^+$ observed at *m/z* 570.

Zinc attaches to the dinucleotides in a manner analogous to that observed for iron. Abundant $(dinucleotide+zinc-3H)^-$ and $(dinucleotide+zinc+DHB-3H)^-$ ions are observed in all cases, except for the dinucleotide *d*CT. In this case, no $(dCT+zinc-3H)^-$ ions were observed at *m/z* 592. Rather, the most abundant ion was $(dCT+zinc+DHB-3H)^-$ at *m/z* 746. This is precisely what is observed for the interaction of iron with *d*CT, and supports the conclusion that a second proton is difficult to abstract from the dCT species to attach the divalent metal ion and eliminate the second molecule of DHB.

Zinc (II) is known to catalyze the hydrolysis of oligonucleotides, presumably through a oligonucleotide–metal ion macrochelate complex [25]. Both Zn (II) and Mn (II) exhibit sequence specific binding in solution for the guanine nucleobases in small oligonucleotides [26]. In order to evaluate the basis for these observations, the interaction of zinc (II) with tetranucleotides was examined. Multiple zinc ions can be attached to a single tetranucleotide. Fig. 4 reveals that up to three zinc ions can be added to *d*ACGT. The inset reveals the measured isotopic distribution for the molecular ions containing two and three zinc atoms. The attachment of three zinc ions must involve coordination to both the phosphate groups and the nucleobases. Scheme 7 presents a possible structure for this species. Fragment ions are observed, which provide some insight into the possible location of the zinc species in the tetranucleotide. For example, loss

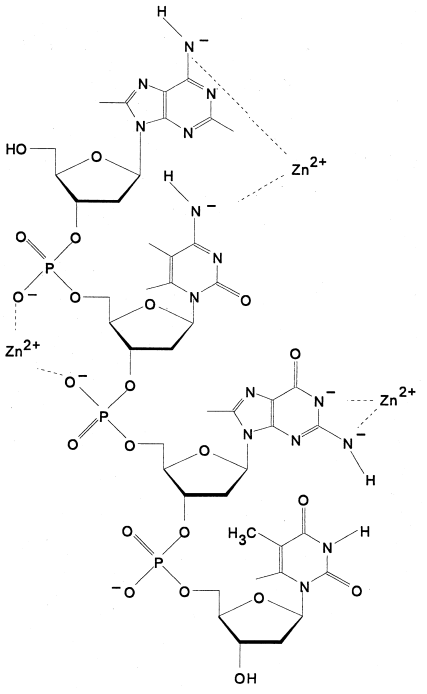

Scheme 7.

of (thymine+water) from the *m/z* 1234 ion of $(d\text{ACGT}+\text{Zn}-3\text{H})^-$ generates a fragment ion at *m/z* 1090, which still contains the zinc atom. This supports the proposition that the zinc ion is not associated closely with the thymine nucleic base. Higher mass ions are also observed in Fig. 4, and correspond to zinc+*d*ACGT+DHB adducts.

3.5. Divalent–trivalent metal ion–oligonucleotide interactions: iron

Ionic iron–oligonucleotide complexes can be made and observed in the gas phase with MALDI FTICR mass spectrometry, and reveal the presence of both Fe^{2+} and Fe^{3+} incorporation into oligonucleotides [18]. In this article, the 5′-phosphorylated trinucleotide p*d*ACA will be used as a model oligonucleotide to compare the coordination of iron with that of higher valence metal ions such as cerium and thorium. Up to two iron ions can be added to p*d*ACA to generate *m/z* 986 and 1040, as shown in Fig. 5. The inset reveals that the first iron ion can be added as either Fe^{2+} (as $(\text{p}d\text{ACA}+\text{Fe}-3\text{H})^-$ at *m/z* 986) or Fe^{3+} (as $(\text{p}d\text{ACA}+\text{Fe}-4\text{H})^-$ at *m/z* 985). High-resolution mass measurement of the *m/z* 1040 ion reveals that this species contains both iron ions exclusively as divalent species (i.e. Fe^{2+}, Fe^{2+}). The fragmentation observed in Fig. 5 reveal that the *m/z* 986 and 1040 ions can dissociate under MALDI conditions to eliminate neutral cytidine to give ions at *m/z* 875 and 929, respectively, which retain the iron ion in each case. Collisional dissociation of $(\text{p}d\text{ACA}+\text{Fe}-3\text{H})^-$ at *m/z* 986 reveals elimination of deoxyadenosine to generate a $(d2+\text{Fe})^-$ fragment ion. For comparison, the SORI-CAD of the $(\text{p}d\text{ACA}-\text{H})^-$ ion at *m/z* 932 for p*d*ACA dissociates under the same excitation conditions to yield fragment ions at *m/z* 797 (elimination of adenine), 699 (elimination of deoxyadenosine), and 619 (*w*2 ion). The formation of *d*-type fragment ions rather than *w*-type fragment ions was also observed in dissociation of iron–phosphorylated tetranucleotide negative ions [18]. Numerous higher mass ions observed in Fig. 5 reveal sequential attachment of either $(Fe^{3+}+\text{DHB})$ or $(Fe^{2+}+\text{DHB})$ to the ions discussed previously.

Although collisional dissociation methods provide some information as to the location of the metal ions in the oligonucleotides, ion–molecule reactions can be used to probe the reactivity of the gas phase metal–oligonucleotide ions and thus provide some detail about the site of metal ion attachment and its accessibility for further reaction. To this end, the *m/z* 986 ion $(\text{p}d\text{ACA}+\text{Fe}-3\text{H})^-$ identified above was reacted with ethylene oxide. This was done to probe if oxygen could be added to the ionic iron present. No reaction was observed, suggesting that the iron ion is solvated extensively within the oligonucleotide, making it inaccessible for further reaction in this particular case.

We have evaluated a range of oligodeoxyribonucleotides to examine the factors that influence how many iron ions can be attached to a given oligomer. Table 3 summarizes the results for several small oligonucleotides up to hexanucleotides. Because each Fe^{2+} addition displaces two protons, it is clear that the multiple metal ion coordination to small oligonucleotides often involves both phosphate and nucleobase binding interactions. The trinucleotides *d*TGT and

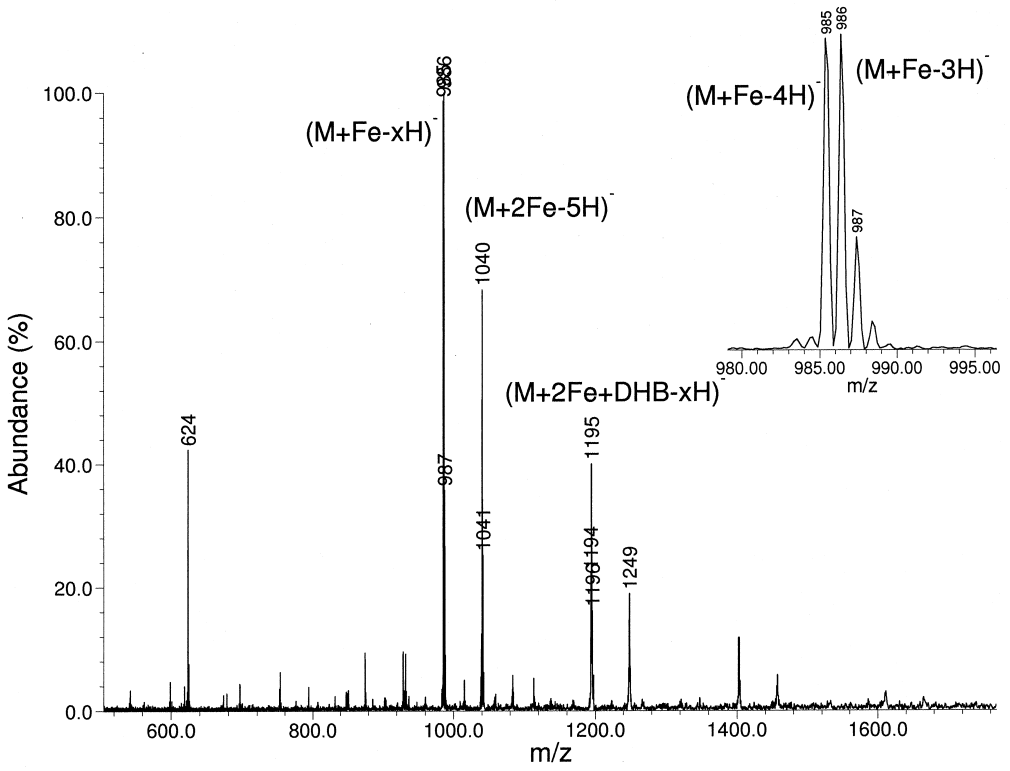

Fig. 5. Negative ion MALDI FTICR mass spectrum of sample containing 2,5-DHB, iron (III) chloride, and p*d*ACA. The insert is an expansion of the $(M+Fe–xH)^-$ ion, revealing the presence of both Fe^{2+} (*m/z* 986) and Fe^{3+} (*m/z* 985) in this species.

Table 3
Iron ion addition to oligonucleotide negative ions[a]

Oligonucleotide	Maximum number of iron ions added
*d*TGT	1
*d*GGT	1
p*d*ACA	2
*d*ACGT	3
*d*AGCT	2
p*d*AGCT	3
p*d*AATT	3
*d*AGCTAG	3

*** Iron (III) chloride was mixed with the aqueous DHB matrix, and then the dinucleotide was added to the solution. The resulting mixture was dried onto the stainless steel probe tip for MALDI-FTICR-MS examination. Each Fe^{2+} added replaces two protons of the dinucleotide; each Fe^{3+} replaces three protons. In every case shown above, the complex with one iron ion corresponded to the presence of both Fe^{3+} and Fe^{2+}, whereas the addition of multiple iron ions always corresponded to the presence of only Fe^{2+} species.

*d*GGT are observed to attach only one iron ion, which can be either Fe^{2+} or Fe^{3+}. Because there is only one nondeprotonated phosphate in the parent negative ion, the iron ion must be coordinated either exclusively to the nucleobase(s) or involve both phosphate and nucleobase deprotonation. Similar structures for metal ion binding to both phosphate and nucleobase groups have been proposed for complexes of platinum (II) with oligonucleotides [27]. Addition of a terminal phosphate group to a trinucleotide provides two additional acidic protons and allows attachment of a second iron ion, as illustrated for p*d*ACA. The first iron to be attached can exist as either Fe^{2+} or Fe^{3+}; however, the attachment of two iron ions to p*d*ACA is possible only if both irons are present as Fe^{2+}. The lack of Fe^{3+} in the *m/z* 1040 ion, along with the inability to attach a third iron ion, provides information about the number and location of abstractable

protons. Two isomeric tetranucleotides were examined for iron attachment. Table 3 reveals that whereas *d*ACGT will attach up to three iron ions, *d*AGCT will attach only two iron ions. Presumably the first iron attached for either tetramer replaces the two acidic protons on the nondeprotonated phosphate groups. The remaining iron ions must coordinate to the nucleobases. For *d*ACGT, one additional Fe^{2+} could be added to tether the cytidine and adenine nucleobases together, as was observed for the dinucleotide *d*CA. The third iron could be attached solely to the guanine nucleobase. For *d*AGCT, the second iron added most likely is associated with the guanine nucleobase. It would be difficult to attach a third iron ion, since the cytidine and adenine nucleobases are physically separated by the guanine. As discussed previously for the trinucleotides, the presence of a terminal phosphate group in a tetranucleotide provides additional protons for attachment of the second iron ion. For example, both p*d*AGCT and p*d*AATT can attach up to three iron ions. The first two iron ions are probably added by replacing the four acidic hydrogens on the phosphate groups. The third iron ion would then add to either the adenine–guanine nucleobases (for p*d*AGCT) or the adenine–adenine nucleobases (for p*d*AATT). Whereas *d*AGCT will attach only up to 2 iron ions, p*d*AGCT can attach an additional iron, likely due to the additional protons provided by the terminal phosphate group. The hexanucleotide *d*AGCTAG was found to attach up to three iron ions in the negative ion mass spectra (with HPA as the matrix compound), and up to four ions in the positive ion mass spectra, as shown in Fig. 6(a) and (b). For this hexanucleotide, up to two Fe^{2+} could be attached to the nondeprotonated phosphate groups present in this negative ion, with the remaining Fe^{2+} ions attached to the nucleobases, especially guanine. Note the abundance of *w*-type fragment ions in Fig. 6, especially in the positive ion mass spectrum, many of which contain one or more iron ions. A few of these iron-containing ions are labeled in the mass spectra.

The strong interaction of iron with oligonucleotides and the ability to attach multiple iron ions to a single oligomer suggest that this metal ion might have application as a selective probe to interrogate oligomer structures. This might be conducted by using the iron ions to probe the presence or absence of acidic hydrogens, and thus the sequence or modification of phosphates and nucleobases in these species.

3.6. Trivalent–tetravalent metal ion–oligonucleotide interactions: cerium and thorium

The presence of Fe^{3+} in metal ion–oligonucleotide adducts suggests that other highly charged metal ions could be coordinated and may provide additional structural information. To investigate this option, research was focused on evaluation of lanthanide and actinide metal ions, which can have trivalent and tetravalent oxidation states. Lanthanides have been determined to be effective for DNA binding and hydrolysis [28], with cerium observed as the most efficient metal ion for this process [29,30].

MALDI FTICR mass spectrometry of the trinucleotide pdACA plus a cerium salt [Ce (III) nitrate] revealed a $(pdACA+Ce-xH)^-$ ion at nominal *m/z* 1069, as shown in Fig. 7. Expansion of the molecular ion region, shown in the insert in Fig. 7, suggests that both Ce^{3+} (as $(pdACA+Ce-4H)^-$ at *m/z* 1069) and Ce^{4+} (as $(pdACA+Ce-5H)^-$ at *m/z* 1068) are present in the metal ion adduct. Fig. 8(a) compares the measured isotopic distribution of the $(pdACA+Ce-xH)^-$ ion with the calculated isotopic distribution, shown in the insert of Fig. 8(a), for $(pdACA+Ce-4H)^-$, which corresponds to only the Ce^{3+} species. The absence of an ion at *m/z* 1068 in the calculated isotopic abundance indicates that the *m/z* 1068 ion observed in Fig. 7 is due to $(pdACA+Ce-5H)^-$, verifying the presence of Ce^{4+} in this species. Whereas the Ce^{3+} ion could simply replace the three remaining acidic phosphate hydrogens of the p*d*ACA negative ion, the incorporation of Ce^{4+} must also involve nucleobase binding. One possible structure for this ion is illustrated in Scheme 8. It is interesting to note that Ce^{4+} has been found to be extremely useful for accelerating nonenzymatic DNA hydrolysis in solution by a factor of 10^{11}-fold or more [29]. An ion appears in Fig. 7 at *m/z* 1160, which cannot be rationalized based on (p*d*ACA+Ce+DHB). High resolution of this species reveals a simple isotopic

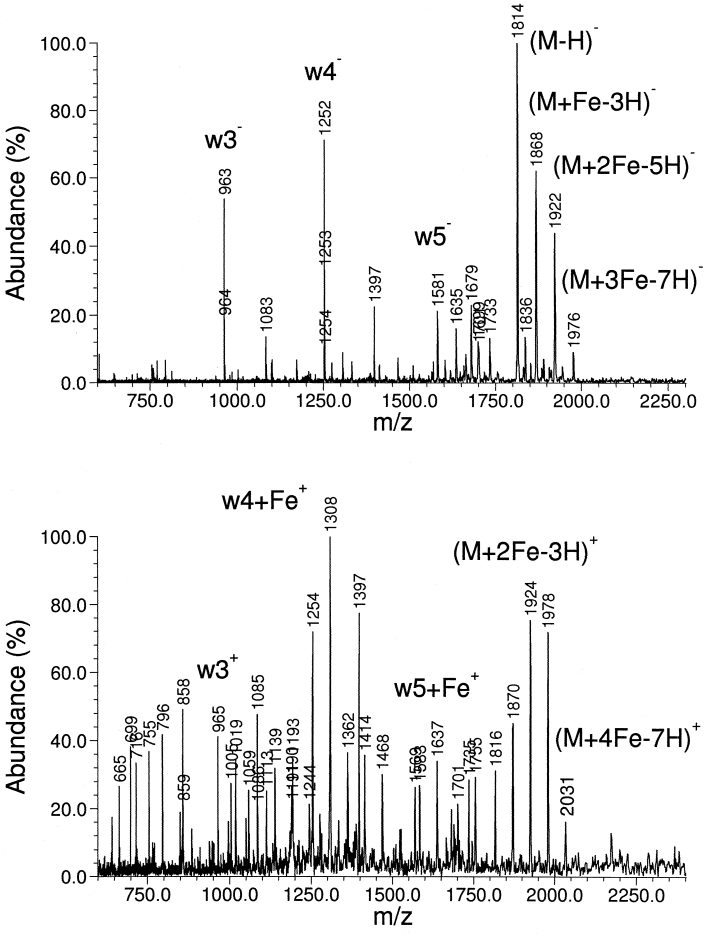

Fig. 6. MALDI FTICR mass spectrum of sample containing 3-HPA, iron (III) chloride, and *d*AGCTAG, under a) negative ions conditions, and b) positive ion conditions. Up to three iron ions can be attached in the negative ion mode, whereas the attachment of up to 4 iron ions is observed in the positive ion mode. See text for details.

signature, shown in Fig. 8(b). Because the sample of cerium (III) nitrate used was at least ten years old and of uncertain purity, an elemental analysis was conducted on the salt. Inductively coupled plasma (ICP) mass spectrometry verified the presence of a few percent (by weight) of thorium in the cerium nitrate sample. This is not unexpected, especially in older purified cerium samples, since thorium occurs naturally with cerium and is difficult to remove due to its chemical properties, which are similar to cerium. Close inspection of the mass spectra suggests that the ion at *m/z* 1160 is due to $(pdACA+Th-5H)^-$, corresponding to Th^{4+} addition to this trinucleotide. The isotopic distribution measured for the *m/z* 1160 ion accurately matches the expected abundance of thorium isotopes, as shown in the inset of Fig. 8(b). Although cerium can exist as either Ce^{3+} or Ce^{4+}, thorium is known to exist only as Th^{4+}. This is reflected accurately in the (p*d*ACA+metal ion) species in Fig. 8(b). The remaining ions in Fig. 7 correspond to DHB adducts of the metal ion–p*d*ACA ions listed above. Each of the parent ions at *m/z* 1069 and 1160 can fragment by loss of neutral cytidine to give fragment ions at *m/z* 958 and 1049, respectively. Both of these ions retain the isotopic signature of the metal, verifying the retention of the metal ion in the fragments. Collisional dissociation experiments of the *m/z* 1069 ion verify the elimination of cytidine as the

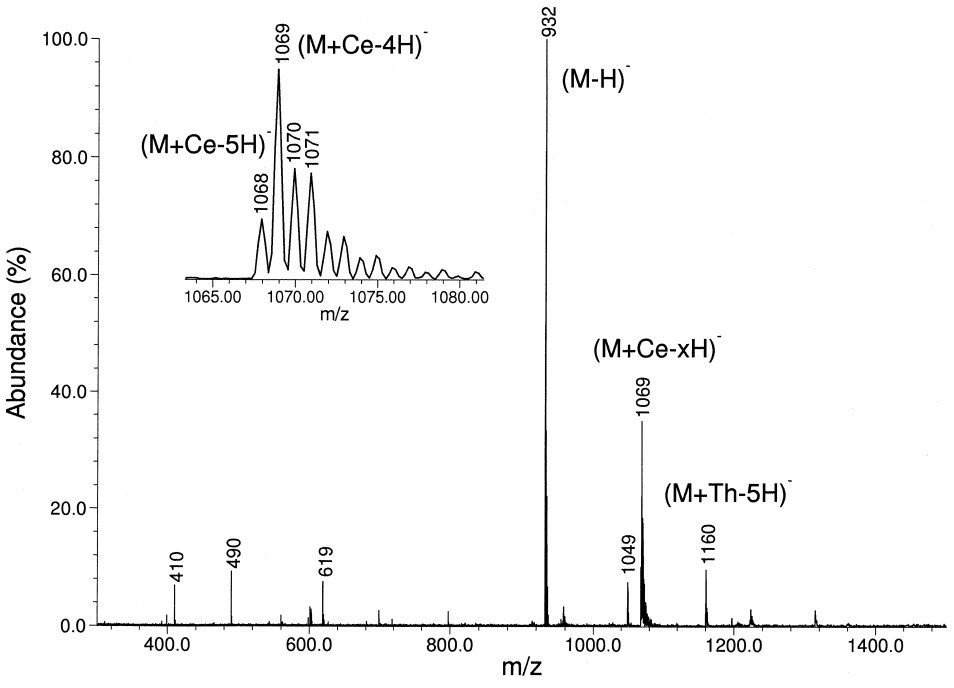

Fig. 7. Negative ion MALDI FTICR mass spectrum of sample containing 2,5-DHB, cerium (III) nitrate, and p*d*ACA. The insert is an expansion of the $(M+Ce-xH)^-$ ion, revealing the presence of both Ce^{3+} (*m/z* 1069) and Ce^{4+} (*m/z* 1068) in this species.

primary dissociation pathway. As stated earlier, this is in contrast to the SORI-CAD of the $(M-H)^-$ ion at *m/z* 932 for p*d*ACA, which fragments primarily by elimination of adenine and deoxyadenosine.

In order to investigate the effect of varying the initial oxidation state of the lanthanide metal, a cerium (IV) salt was employed in the sample preparation. This $Ce(NH_4)_4(SO_4)_4$ was dissolved in water and mixed with the aqueous DHB matrix compound prior to introduction of the pdACA trinucleotide into the solution. MALDI FTICR mass spectra of this sample also revealed $(pdACA+Ce-4H)^-$ at *m/z* 1069, as shown in Fig. 9(a). However, expansion of the molecular ion region, shown in Fig. 9(b), reveals that only Ce^{3+} is present in the metal ion adduct. This is determined by the absence of the *m/z* 1068 that was observed in Fig. 7, and by good agreement between the measured isotopic distribution of Fig. 9(b) and the calculated isotopes in the insert of Fig. 8(a). The presence of only Ce^{3+} in Fig. 9 is unexpected, since the Ce (III) nitrate salt generated both Ce^{3+} and Ce^{4+} complexes. Fig. 10(a) reveals the mass spectrum obtained when the abundant $(M-H)^-$ ion at *m/z* 932 for p*d*ACA was ejected prior to ion detection. Note the appearance of $(pdACA+Fe-xH)^-$ at nominal *m/z* 986, highlighted in the expansion of Fig. 10(b). It appears that the Ce(IV) salt has oxidized the stainless steel probe tip to leach ionic iron into the MALDI sample, which is then reflected by the presence of iron adducts in the mass spectra. This would result in a reduction of the Ce (IV) to Ce (III), which is also reflected in the mass spectra. The Ce(IV) salt may also oxidize the MALDI matrix compound, DHB, to form a quinone-type structure, also resulting the reduction of Ce (IV) to Ce (III). This cerium sample apparently was devoid of thorium contamination, since no characteristic thorium ions were observed in the mass spectra.

Cerium and thorium adducts of tetranucleotides can also be generated with the cerium nitrate salt. MALDI mass spectra of cerium (III) nitrate mixed with the tetranucleotide *d*ACGT results in the addition of only one cerium or one thorium to give ions at *m/z*

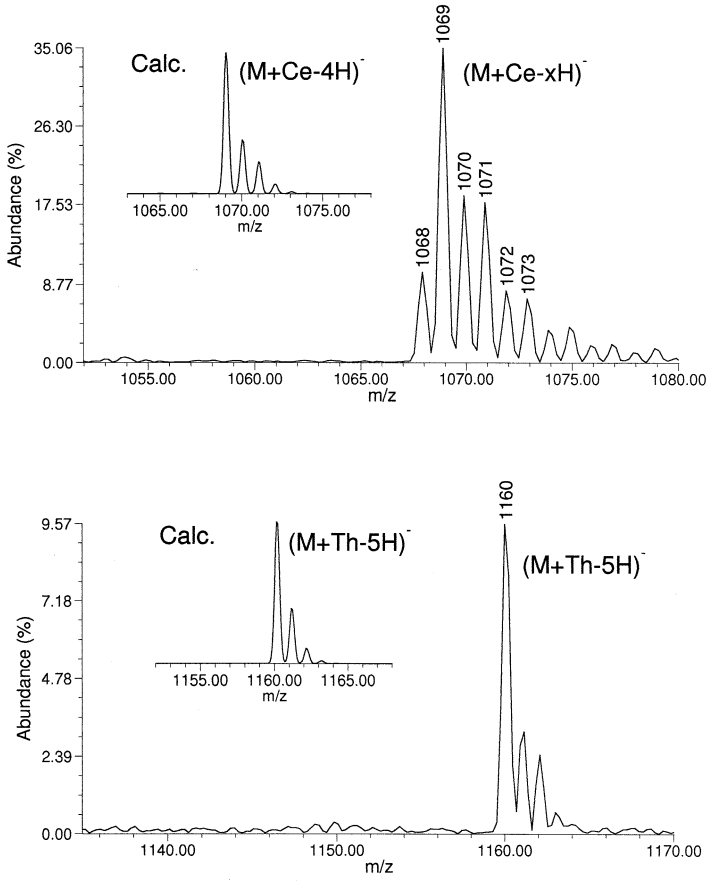

Fig. 8. Comparison of measured negative ion mass spectra with calculated theoretical isotopic distributions for a) the $(M+Ce-xH)^-$ ion at nominal *m/z* 1069 from Figure 7, and b) the $(M+Th-xH)^-$ ion at nominal *m/z* 1160 from Figure 7.

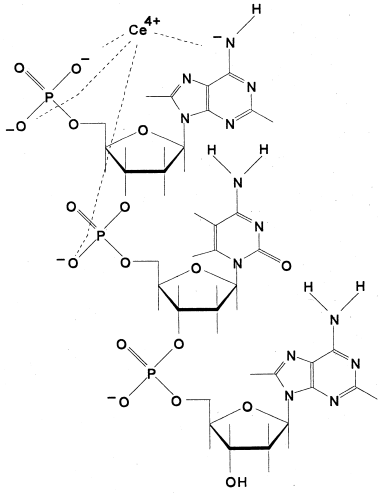

Scheme 8.

1308–1309 $(d\text{ACGT}+Ce-xH)^-$ and *m/z* 1400 $(d\text{ACGT}+Th-5H)^-$. Expansion of the mass range in the *m/z* 1300–1325 region reveals both $(d\text{ACGT}+Ce-4H)^-$ and $(d\text{ACGT}+Ce-5H)^-$, verifying the presence of Ce^{3+} and Ce^{4+} in these complexes. As expected, the *m/z* 1400 ion corresponds exclusively to $(d\text{ACGT}+Th-5H)^-$, in which Th^{4+} is present. The *m/z* 1309 ion can fragment by losing either cytidine or thymine to yield fragment ions which retain the isotopic signature of the cerium atoms.

With terminally phosphorylated tetranucleotides, such as p*d*AGCT, the use of the cerium nitrate salt generated only thorium–tetranucleotide adducts, with $(pd\text{AGCT}+Th-5H)^-$ observed as the most abundant

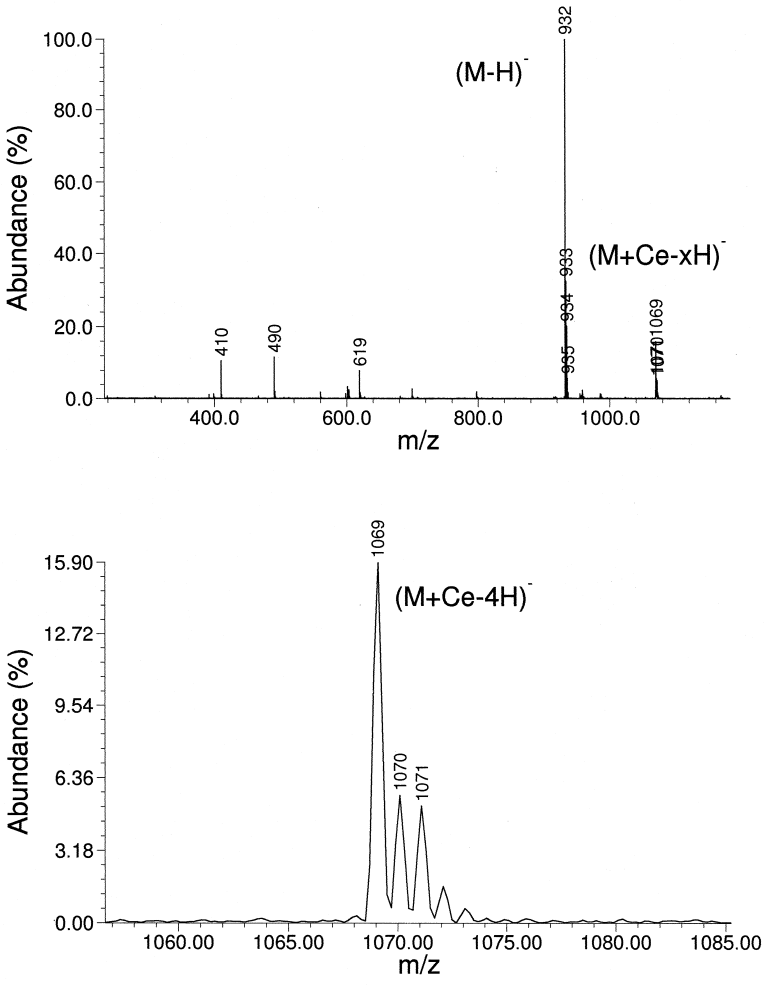

Fig. 9. Negative ion MALDI FTICR mass spectrum of sample containing 2,5-DHB, cerium (IV) ammonium sulfate, and p*d*ACA. The entire mass spectrum is shown in a), while an expansion of the *m/z* 1055-1085 region is shown in b), illustrating the presence of only Ce^{3+} in this ion.

species. Even though thorium in only present in the sample at a few percent, the availability of sufficient acidic hydrogens on the phosphorylated tetranucleotide enhances the production of the thorium adducts over the cerium species. Changing to the Ce (IV) salt with the same p*d*AGCT tetranucleotide revealed $(pdAGCT+Ce-4H)^-$ at *m/z* 1389 (presence of Ce^{3+} only) and $(pdAGCT+Fe-xH)^-$ at *m/z* 1305–1306 (presence of Fe^{2+} and Fe^{3+}). These species fragment by loss of (thymine+water).

These results with cerium and thorium reveal that multivalent metal ions have strong affinities for oligonucleotides. The metal bonding in these cases, which may be mostly covalent in nature, involves both phosphate and nucleobase interactions. It is likely that the resulting metal ion–oligonucleotide structure is dictated by the ability of the oligonucleotide to "wrap around" and effectively solvate the multiply charged metal ion, possibly through salt-bridge type structures. This proposal is based on the implication of salt-bridge structures as the stabilizing force for alkali metal ion–nucleobase interactions [31]. The stabilities of metal ion–oligonucleotide systems is confirmed by the fragmentation products,

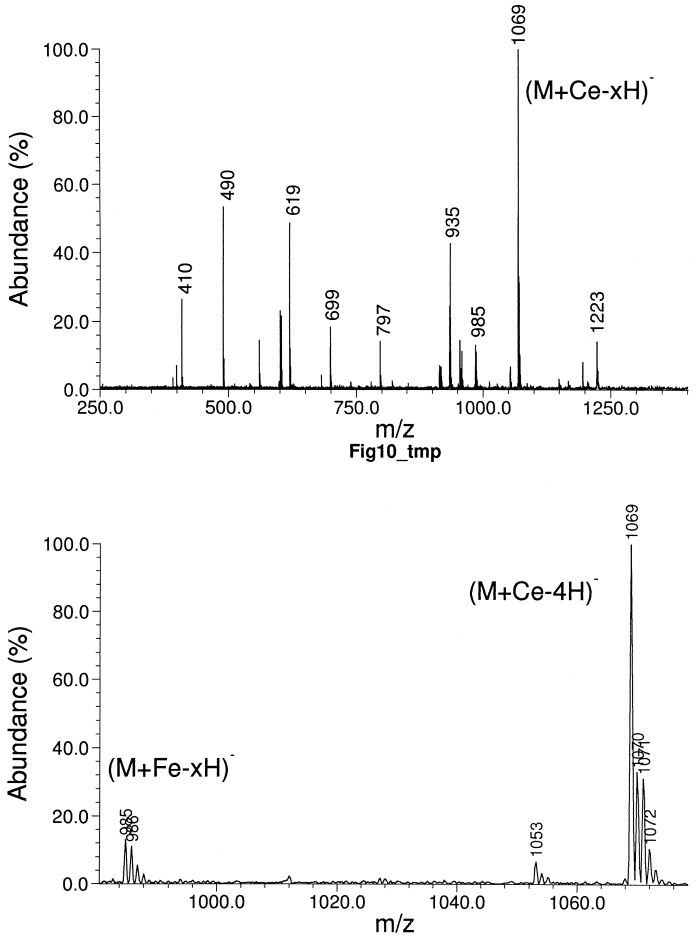

Fig. 10. Same as Figure 9, except the abundant *m/z* 932 was ejected prior to ion detection. The entire mass spectrum is shown in a), while the expanded *m/z* 980–1080 region in b) reveals the presence of $(M+Fe-xH)^-$ for this sample.

which reveal loss of pyrimidine nucleobases in general, with the metal ion retained in the fragment ions.

4. Conclusions

MALDI FTICR mass spectrometry is a powerful technique for examination of the fundamental interactions of metal ions with small oligonucleotides. The capabilities of this technique for accurate mass measurement under medium-high resolution conditions and ion manipulation to probe fragmentation products can be used to interrogate the identities and structures of gas phase metal ion–oligonucleotide complexes. By systematically varying either the identity of the metal ion or the sequence of a dinucleotide, it was possible to examine the influence of the nucleobase sequence on the attachment of copper and iron ions. Copper (I) attachment probes the maximum number of protons that can be replaced by a singly charged metal ion, whereas iron attachment is sensitive also to steric factors (i.e. attachment to multi sites within the dinucleotide). Based on this data, a mechanism for metal ion–oligonucleotide formation was proposed in which the (metal ion–DHB) complexes react with the oligonucleotides to attach the metal concomitant with elimination of a DHB molecule. The attachment of multiple iron ions to oligonucleotides was found to be strongly influenced by not only the number of nondeprotonated phosphate groups, but also the sequence order of the nucleobases in the oligonucleotide. Lan-

thanide and actinide ions interact strongly with oligonucleotides and reveal that highly charged metal ions such as Ce^{4+} and Th^{4+} bind strongly to these biomolecules and are retained even in the fragmentation process. These studies provide molecular level information about the fundamental nature of metal ion interactions with oligonucleotides, which may enable the determination of how such a metal ion system could be exploited as selective probes for biomolecule interrogation.

Acknowledgements

Acknowledgment is given to Dr. Doug Duckworth (ORNL) for the ICP mass spectra measurements of the cerium nitrate sample, and to the Office of Biological and Environmental Sciences, Department of Energy for support of this research at Oak Ridge National Laboratory under contract no. DE-AC05-96OR22464 with Lockheed Martin Energy Research, Inc.

References

[1] A. Hartwig, L. Mullenders, M. Asmuss, H. Dally, M. Hartmann, Fresenius J. Anal. Chem. 361 (1998), 377.
[2] P.D. Boyer, Biochemistry 26 (1987), 8503.
[3] F.H. Westheimer, Science 235 (1987), 1173.
[4] H. Sigel, in Metal-DNA Chemistry, T.D. Tullius (Ed.), ACS Symposium Series 402, American Chemical Society, Washington, DC, 1989, p. 159.
[5] C.S. Garland, E. Tarien, R. Nirmala, P. Clark, J. Rifkind, G.L Eichhorn, Biochemistry 38 (1999) 3421.
[6] J.K. Barton, S.J. Lippard, in Nucleic Acid–Metal Ion Interactions, T.G. Spiro (Ed.), Wiley, New York, 1980, p. 31.
[7] E.S. Henle, Z.X. Han, N. Tang, P. Rai, Y.Z. Luo, S. Linn, J. Biol. Chem. 274 (1999) 962.
[8] J.W. Sam, S. Takahashi, I. Kippai, J. Peisach, D.L. Rousseau, J. Biol. Chem. 273 (1998) 16090.
[9] E.S. Henle, Y.Z. Luo, W. Gassmann, S. Linn, J. Biol. Chem. 271 (1996) 21177.
[10] R.M. Burger, Chem. Rev. 98 (1998) 1153.
[11] V.A. Bloomfield, D.M. Crothers, I. Tinoco Jr., Physical Chemistry of Nucleic Acids, Harper and Row, New York, 1974, p. 420.
[12] N.G.A. Abrescia, L. Malinina, L.G. Fernandez, T. Huynh-Dinh, S. Neidle, J.A. Subirana, Nucl. Acids Res. 27 (1999) 1593.
[13] L.G. Marzilli, T.J. Kistenmacher, G.L. Eichhorn, in Nucleic Acid–Metal Ion Interactions, T.G. Spiro (Ed.), Wiley, New York, 1980, p. 179.
[14] J.A. Loo, Mass Spectrom. Rev. 16 (1997) 1.
[15] E.A. Stemmler, R.L. Hettich, G.B. Hurst, M.V. Buchanan, Rapid Commun. Mass Spectrom. 7 (1993) 828.
[16] N.P. Christian, S.M. Colby, L. Giver, C.T. Houston, R.J. Arnold, A.D. Ellington, J.P. Reilly, Rapid Commun. Mass Spectrom. 9 (1995) 1061.
[17] N.P. Christian, L. Giver, A.D. Ellington, J.P. Reilly, Rapid Commun. Mass Spectrom. 10 (1996) 1980.
[18] R.L. Hettich, J. Am. Soc. Mass Spectrom. 10 (1999) 941.
[19] J.A. Castoro, C. Koster, C. Wilkins, Rapid Commun. Mass Spectrom. 6 (1992) 239.
[20] J.W. Gauthier, T.R. Trautman, D.B. Jacobson, Anal Chim. Acta. 246 (1991) 211.
[21] T. Kojima, I. Kudaka, T. Sato, T. Asakawa, R. Akiyama, Y. Kawashima, K. Hiraoka, Rapid Commun. Mass Spectrom. 13 (1999) 2090.
[22] A.T. Blades, P. Jayaweera, M.G. Ikonomou, P.Kebarle, Int. J. Mass Spectrom. Ion Processes 101 (1990) 325.
[23] P. Jayaweera, A.T. Blades, M.G. Ikonomou, P. Kebarle, J. Am. Chem. Soc. 112 (1990) 2452.
[24] M.A. Freitas, S.D.-H. Shi, C.L. Hendrickson, A. G. Marshall, J. Am. Chem. Soc. 120 (1998) 10187.
[25] S. Kuusela, H. Lonnberg, Nucleosides Nucleotides 17 (1998) 2417.
[26] M. Montrel, V.P. Chuprina, V.I. Poltev, W. Nerdal, E. Sletten, J. Biomol. Struct. Dynam. 16 (1998) 631.
[27] C.E. Costello, K.M. Comess, A.S. Plaziak, D.P. Bancroft, S.J. Lippard, Int. J. Mass Spectrom. Ion Processes 122 (1992) 255.
[28] R. Hettich, H.J. Schneider, J. Chem. Soc. Perkin Trans. 10 (1997) 2069.
[29] M. Komiyama, N. Takeda, H. Shigekawa, Chem. Commun. (1999) 1443.
[30] R. Ott, R. Kramer, App. Microbiol. Biotech. 52 (1999) 761.
[31] B.A. Cerda, C. Wesdemiotis, J. Am. Chem. Soc. 118 (1996) 11884.